

## Mesoscopic photovoltaic effect in GaAs/Ga<sub>1-x</sub>Al<sub>x</sub>As Aharonov-Bohm rings

L. Angers, A. Chepelianskii, R. Deblock, B. Reulet, and H. Bouchiat  
*Université Paris-Sud, CNRS, UMR 8502, F-91405 Orsay Cedex, France*

(Received 6 April 2007; revised manuscript received 18 May 2007; published 16 August 2007)

When submitted to a high-frequency radiation at low temperature, a mesoscopic conductor develops a sample specific dc voltage. We have investigated this photovoltaic (PV) effect on GaAs/Ga<sub>1-x</sub>Al<sub>x</sub>As Aharonov-Bohm rings at temperatures varying between 30 mK and 1 K. The rf induced PV voltage is a purely mesoscopic effect which exhibits both periodic and aperiodic magnetic flux dependences with zero average value. The harmonics content and symmetry of this flux dependent PV voltage close to zero field depend on the radiation frequency compared to the inverse diffusion time around the sample. The frequency dependence also exhibits sharp resonances which position sign and amplitude strongly depend on magnetic field. We attribute these resonances to the presence of two level systems at resonance with the frequency of the electromagnetic field.

DOI: [10.1103/PhysRevB.76.075331](https://doi.org/10.1103/PhysRevB.76.075331)

PACS number(s): 73.50.Pz, 05.70.Ln, 72.20.My

### I. INTRODUCTION

In mesoscopic systems at low temperature, electrons keep their phase coherence over the whole sample size. Transport and thermodynamic properties are sensitive to interferences between electronic wave functions and exhibit spectacular signatures of this phase coherence. Among them are sample specific universal conductance fluctuations (UCFs) giving rise to reproducible magnetoresistance patterns called magnetofingerprints, which in a ring geometry are modulated by the flux periodic Aharonov-Bohm (AB) oscillations.<sup>1</sup> Besides these effects in the linear transport, it has been shown that phase coherent mesoscopic systems present remarkable rectifying properties related to the absence of spatial inversion symmetry of the disorder potential. This gives rise to a quadratic term<sup>2</sup> in the  $I(V)$  relation:  $I = G_1 V + G_2 V^2$ . When a mesoscopic system is excited by an ac bias voltage, the nonlinear conductance coefficient  $G_2(\omega)$  can be measured by detecting the second harmonics on the current response. This has been done at low frequency.<sup>3-6</sup> On the other hand, at high-frequency bias excitation, the investigation of second order nonlinear transport is generally done by measuring the dc induced signal sometimes called photovoltaic effect which has also given rise to a number of experimental<sup>7-9</sup> and theoretical investigations.<sup>10-13</sup> This quantity has been shown to exhibit characteristic mesoscopic fluctuations. Its sign and amplitude strongly depend on the magnetic field in a similar way as the linear conductance leading to sample specific magnetofingerprints. The frequency dependence, even though less studied, is also expected to exhibit fluctuations with a typical correlation frequency  $f_c = 1/2\pi\tau_D$ , where  $\tau_D = L^2/D$  is the diffusion time around the sample of size  $L$  and  $D$  is the diffusion coefficient. The quantitative interpretations of these experiments are delicate since it is difficult to perfectly control the high-frequency environment of a mesoscopic sample.

The next section is devoted to the theoretical expectations concerning the different contributions to this effect at low and high frequencies compared to  $f_c$ . In this section, completed by the Appendix, we also give a semiclassical derivation of the photovoltaic (PV) current valid at frequencies up

to  $f_c$ . We do not consider effects such as modulation of internal parameters of the mesoscopic sample also discussed in Ref. 13 (such as electron density, or shape) with the high-frequency radiation.

We then present in the third section measurements of the photovoltaic effect on individual AB rings fabricated from a bidimensional electron gas in a GaAs/Ga<sub>1-x</sub>Al<sub>x</sub>As heterostructure. The rings were irradiated through an antenna with a radio frequency field whose frequency varies between 1 and 18 GHz. The antenna is located far enough from the sample in order that any gating effect can be neglected. We find that the field dependence of PV voltage detected between two wires attached to a ring exhibits (AB) oscillations and aperiodic fluctuations. Both quantities decay with temperature on a scale related to the inverse diffusion time through the rings and depend nonmonotonously on the rf injected power, in agreement with theoretical predictions.

In Sec. IV, we discuss the field asymmetry of the photovoltaic effect. We find that it exhibits even and odd components in magnetic field which are of the same order of magnitude at large field scale. This effect was already observed in the dc rectification of AB rings and related to electron-electron (e-e) interactions.<sup>6</sup> In contrast, the behavior of the AB oscillations is more subtil, just like in the dc limit (see Ref. 6), they exhibit either a maximum or a minimum at zero field up to  $f = f_c/2$ , i.e., their phase is either equal to 0 or  $\pi$ . On the other hand, this phase takes random values at higher-frequencies. We attribute this effect to the time reversal symmetry breaking induced by the high-frequency electric field experienced by an electron diffusing around the ring on the time scale  $\tau_D$ , in agreement with predictions of Sec. I. In the same frequency range below  $f_c$ , we observe an increase of the  $\phi_0/2$  periodic component of the PV voltage.

Finally, in Sec. V, we compare the frequency dependence to theoretical predictions. We also show evidence of strong variations of the PV voltage as a function of frequency which can be at first approximation related to the frequency dependent electromagnetic environment of the rings. However, inside the rather broad peaks which can be directly attributed to the resonances of the high-frequency setup, we could also detect narrow peaks whose amplitude and position depend on magnetic field. We attribute them to the existence of two

level systems (TLSs) at resonance with the frequency of the electromagnetic field. When associated with scattering impurities coupled with the conduction electrons, these TLSs give rise to oscillating dipoles whose amplitude goes through a maximum at their resonance frequencies. They strongly affect the second order voltage response at these particular frequencies and can be detected on the photovoltaic response.

## II. MESOSCOPIC PHOTOVOLTAIC EFFECT: ORDERS OF MAGNITUDE AND BASIC THEORETICAL EXPECTATIONS

The aim of this section is to present a semiclassical derivation of the PV current which validity is limited to  $f \leq f_c = 1/2\pi\tau_D$ . We start from the Büttiker-Landauer expression of the linear conductance of a mesoscopic system between two reservoirs:  $G = (T_{12} + T_{21})/2$  where  $T_{12}$  and  $T_{21}$  are the transmission coefficients from reservoir 1 to reservoir 2 and vice versa. In the semiclassical approximation ( $k_F l_e \gg 1$ ), it is possible to express these transmission coefficients at zero temperature in terms of interferences:

$$\begin{aligned} T_{12} &= 2\sum_{i,j} A_i A_j \cos[\phi_i(B) - \phi_j(B)], \\ T_{21} &= 2\sum_{i,j} A_i A_j \cos[\phi_{-i}(B) - \phi_{-j}(B)], \end{aligned} \quad (1)$$

between scattering electronic waves characterized by their amplitudes  $A_i = A_{-i}$  and phase factors  $\phi_i, \phi_{-i}$ , where indexes  $i, j$  run on all pairs of possible trajectories going from 1 to 2 as well as their time reversed  $-i, -j$ . As a result, the conductance can be written as

$$G = 2\sum_{i,j} A_i A_j \cos\left(\frac{\phi_{ij} + \phi_{-ij}}{2}\right) \cos\left(\frac{\phi_{ij} - \phi_{-ij}}{2}\right), \quad (2)$$

where  $\phi_{ij} = \phi_i - \phi_j$  and  $\phi_{-ij} = \phi_{-i} - \phi_{-j}$ .  $\phi_{ij}(B)$  and  $\phi_{-ij}(B) = \phi_{ij}^0 \pm 2\pi B S_{ij}/\Phi_0$ , where  $S_{ij} = -S_{ji}$  is the algebraic surface comprised between trajectories  $i$  and  $j$ . In particular, according to Onsager symmetry rules  $\phi_{-i}(B) = \phi_i(-B)$  so that the magnetoconductance takes the following form:

$$G = 2\sum_{i,j} A_i A_j \cos(\phi_{ij}^0) \cos(2\pi B S_{ij}/\Phi_0), \quad (3)$$

where the zero magnetic field time reversal symmetry invariant phase factors are identical to<sup>14</sup>

$$\phi_{ij}^0 = \phi_{ij}(B=0) = \phi_{-ij}(B=0) = \int_i - \int_j \frac{1}{\hbar} U(r(\vec{r})) dt, \quad (4)$$

with  $U(\vec{r}) = E_F + eV_{dis}(\vec{r})$ , assuming that the disordered potential  $V_{dis}(\vec{r})$  varies slowly on the electron Fermi wavelength which is a reasonable assumption in a two-dimensional electron gas.

In the presence of a time dependent potential  $V(\vec{r}, t) = V(\vec{r})\cos(\omega t)$  applied to the sample and neglecting electron-electron interactions, one can assume that the phase accumulated along a trajectory  $i$  or  $-i$  is modified according to the integral

$$\delta\phi_i(t) = \int_i (1/\hbar) V(r(\vec{r}), t) dt. \quad (5)$$

This leads to an estimate of the photovoltaic current:

$$I_{PV} = \langle \delta G(V(t)) V(t) \rangle_t, \quad (6)$$

where  $\delta G(V(t)) = \sum_{ij} (\partial G / \partial \phi_{ij}) \delta\phi_{ij}(t) + \dots$  (idem with  $-i, -j$ ) is the time dependent correction to  $G$  induced by the rf voltage  $V(t)$ . These phase factors are identical to zero when there is no spatial dependence of the potential in the sample (see the Appendix). In this approximation, where the frequency dependence of the linear conductance is neglected, it is possible to decompose  $I_{PV}$  into two contributions which are symmetric and antisymmetric versus time reversal symmetry:  $I_{PV} = I_{PV+} + I_{PV-}$  with

$$I_{PV+} = \sum_{i,j} A_i A_j \sin(\phi_{ij}^0) \cos(\alpha_{ij} B) \langle [\delta\phi_{ij}(t) + \delta\phi_{-i-j}(t)] V(t) \rangle_t, \quad (7)$$

$$I_{PV-} = \sum_{i,j} A_i A_j \cos(\phi_{ij}^0) \sin(\alpha_{ij} B) \langle [\delta\phi_{ij}(t) - \delta\phi_{-i-j}(t)] V(t) \rangle_t, \quad (8)$$

where  $\alpha_{ij} = 2\pi S_{ij}/\Phi_0$ . In the quasistatic limit  $\omega\tau_D \ll 1$ , one can neglect the time dependence of the potential on the time scale of the diffusive trajectory  $\delta\phi_{ij}(t) = \delta\phi_{-ij}(t) \simeq eV \cos(\omega t) (\tau_i - \tau_j)/\hbar$ , where  $V \cos(\omega t)$  is the spatial average drop of the bias potential on the diffusive mesoscopic sample considered and  $\tau_i$  is the time scale associated with the diffusive trajectories  $i$  and  $-i$ . This yields the static result<sup>2</sup>  $I_{PV-} = 0$  and the typical value of the PV current:

$$I_{PV}(f=0) = I_{PV+}^{LF} \sim (e/\tau_D)(eV\tau_D/\hbar)^2. \quad (9)$$

The PV voltage in this static limit and in the absence of electron-electron interactions is an even function of magnetic field.

At high frequency, one cannot neglect the time dependence of the potential on the diffusive trajectories. As shown in Ref. 15 contrary to a static potential, a time dependent potential breaks time reversal symmetry, giving rise to a phase difference between time reversed trajectories  $i$  and  $-i$ :

$$\begin{aligned} \delta\phi_{i,-i}(t, \tau_i) &= \delta\phi_i - \delta\phi_{-i} \\ &= (e/\hbar) \int_t^{t+\tau_i} V(\vec{r}(\tau), \tau) d\tau - V(\vec{r}(\tau_i - \tau), \tau) d\tau. \end{aligned} \quad (10)$$

The calculation of  $\delta\phi_{i,-i}$  detailed in the Appendix of the paper is inspired by Ref. 15. We find that, in the limit where  $\omega\tau_D \ll 1$ ,  $\delta\phi_{i,-i}$  has a contribution in first order in  $\omega\tau_D$  whose typical value is  $\delta\phi_{i,-i}^{1st} = eV(\tau_D/\hbar)\omega\tau_D$ . This contribution is proportional to  $\sin \omega t$ , i.e., out of phase with the ac potential  $V(t)$  and does not contribute to the PV effect according to Eq. (9) where we have neglected the imaginary component of the conductance.<sup>16</sup> We find that  $\delta\phi_{i,-i}$  has also second order contributions in  $(\omega\tau_D)^2$  which are proportional to  $\cos \omega t$  and contribute to the PV voltage. This second contribution  $I_{PV-}$  to the PV current related to time reversal symmetry breaking

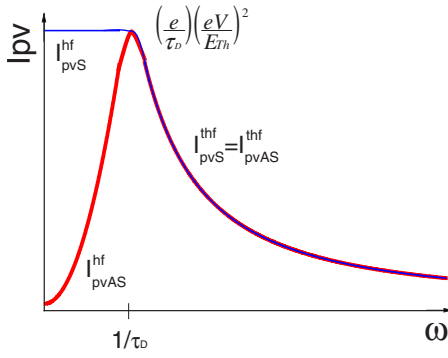


FIG. 1. (Color online) Expected frequency dependence of the components  $I_{PV+}$  and  $I_{PV-}$  of the PV current.

is, according to Eq. (9), an odd function of flux. The typical value of  $I_{PV-}$  is

$$I_{PV-} = V(\partial G/\partial \Phi)_{typ} \delta \phi_{i,-i}^{typ} \sim I_{PV+}(\omega \tau_D)^2. \quad (11)$$

$I_{PV-}$  becomes of the order of  $I_{PV+}$  at  $\omega \tau_D \approx 1$ . Since it is an odd function of magnetic flux near zero field, we expect the phase rigidity of the Aharonov-Bohm oscillations at zero field to disappear in this frequency range. These expressions for the PV current are valid in the limit where  $eV < \hbar/\tau_D$ , the Thouless energy. The PV current goes through a maximum  $I_{PV}^{max} = e/\tau_D$  for  $eV = \hbar/\tau_D$  and is expected to decrease at higher excitation voltage also with contributions due to dephasing effects which are specially important when  $\omega \approx 1/\tau_D$ .<sup>15,18,19</sup>

In the limit where  $\omega \tau_D \gg 1$ , the typical values of phase factors  $\delta \phi_{i,j}$  and  $\delta \phi_{i,-i}$  are both of the order of  $eV/\hbar \omega$  (see the Appendix). In this frequency range, the amplitude of the conductance fluctuations is given by  $e^2/(\hbar \sqrt{\omega \tau_D})$ .<sup>19</sup> The factor  $(\omega/\tau_D)^{1/2}$  is due to energy averaging on the energy scale  $\hbar \omega$  and reflects the signature of the rigidity of the spectrum of a diffusive mesoscopic system on the scale of the Thouless energy. This leads to a scaling behavior compatible with the results obtained in Refs. 8 and 10 by a rigorous analysis using the Keldysh formalism

$$I_{PV+}^{HF} \sim e(\omega/\tau_D)^{1/2}(eV/\hbar \omega)^2, \quad (12)$$

$$I_{PV-}^{HF} \sim I_{PV+}^{HF}. \quad (13)$$

Moreover, the symmetric and antisymmetric components of the PV voltage are expected to be of the same order of magnitude in this high-frequency regime (see Fig. 1). This result again is valid only in the low excitation voltage limit because of rf induced dephasing<sup>15,18</sup> and heating effects at high excitation. This generation of a PV voltage odd in magnetic field presents some similarities with the generation of a dc circulating current odd function of dc magnetic field in an isolated AB ring submitted to a high-frequency oscillating flux as pointed out in Ref. 17. However, such circulating currents cannot be detected in the experimental setup described in the next section.

We conclude this section by recalling that the above results are complicated by the existence of electron-electron Coulomb interactions. They strongly modify the potential

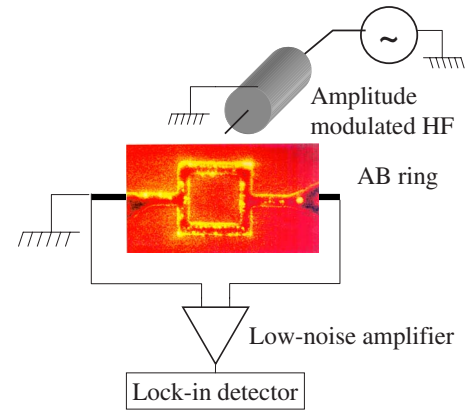


FIG. 2. (Color online) Sketch of the experimental setup used for measuring the PV effect on the ring.

landscape in the mesoscopic system which becomes field dependent without any particular field symmetry. These interactions were thus shown to give rise to a field asymmetry in the second order conductance both theoretically<sup>20-22</sup> and experimentally.<sup>3-5</sup> Nonlinear transport measurements in the very low frequency regime<sup>6</sup> on rings similar to the one investigated here have shown that the magnetic dependence of the second order conductance  $G_2$  does exhibit a magnetic field asymmetry on the large field scale. However, it is still an even function of flux in the vicinity of zero flux due to a strong modulation effect of AB oscillations by low-frequency UCF components. In particular, we have found that the phase of the AB oscillations was either 0 or  $\pi$  at zero magnetic field. As a result, we expect that finite frequency effects on the field asymmetry of the PV voltage will be visible only in this very low field regime where the phase of the Aharonov-Bohm oscillations is still rigid at low frequency even in the presence of Coulomb interactions.

### III. PV EFFECT ON A SINGLE RING: BASIC EXPERIMENTAL RESULTS

A schematic picture of the experimental setup is shown in Fig. 2. The GaAs/Ga<sub>1-x</sub>Al<sub>x</sub>As mesoscopic ring is thermally anchored to the mixing chamber of a dilution refrigerator whose base temperature is 20 mK. The sample is submitted to a high-frequency radiation emitted by a 3 mm long antenna terminating a 50  $\Omega$  cryogenic coaxial cable connected to a generator. The coupling between high-frequency electromagnetic field and the sample is frequency dependent due to attenuation of the cables and the presence of broad resonances in the cables and the copper shield surrounding the sample. It is possible to estimate this frequency dependent coupling by measuring the modification of the linear resistance of the samples heated at high irradiation power as a function of frequency. We find that the effects of the frequency dependent attenuation of the cables and electric coupling to the sample nearly compensate each other so that the rf power sent to the sample only slightly depends on frequency in the range explored in this experiment (from 1 to 17 GHz) on the resonances of the cable. The power at the sample level on these resonances was estimated from the

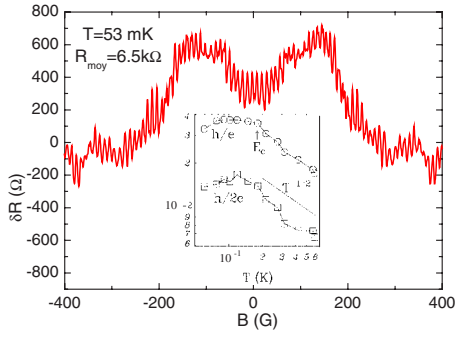


FIG. 3. (Color online) Linear magnetoresistance of the ring measured at low frequency (37 Hz) in a two probe experiment. Inset: Temperature dependence of the  $h/e$  and  $h/2e$  components of the AB oscillations extracted from the Fourier transform of the signal.

observation of Shapiro steps in an ac Josephson experiment performed on a superconducting tunnel junction and found to be of the order of 30 dB lower than the power at the generator level. It is also possible, by detecting the effect of heating on the linear resistance of the sample measured at low frequency, to know within a numerical factor the frequency dependence of the rf voltage applied to the sample.

The amplitude of the high-frequency signal is modulated at low frequency between 37 and 500 Hz. The rectified voltage across the sample is amplified by a low-noise amplifier and measured by a lock-in detector working at the frequency of the amplitude modulation. No dc current is injected in the sample during these photovoltaic effect measurements.

The sample investigated is a square ring (1.5  $\mu\text{m}$  side) etched in a high-mobility two-dimensional electron gas. This ring is in the diffusive regime and contains only a few conducting channels with a dimensionless conductance which varies typically between 2 and 5. There is no electrostatic gate on these samples. Moreover, knowing the typical response of such a sample to a nearby gate, we think that it is safe to neglect any spurious type of gating leading to pumping effects<sup>23</sup> generated by the high-frequency irradiation as investigated in Ref. 24. The linear magnetoconductance of the sample measured with two wires at low temperature (see Fig. 3) exhibits magnetoconductance fluctuations strongly modulated by Aharonov-Bohm  $h/e$  periodic oscillations which are symmetric in magnetic field according to Casimir-Onsager symmetry rules.<sup>25</sup> From these measurements, we extract the characteristic parameters of the ring (see Table I).

The PV voltage measured on the same ring at several rf excitation frequencies is shown in Fig. 4. It strongly varies both in sign and amplitude with magnetic field around a zero average value. This clearly indicated the mesoscopic origin of this PV voltage. The magnetic field dependence of the PV voltage is reproducible for a given frequency but strongly differs from one frequency to the other. They exhibit  $h/e$  periodic AB oscillations modulated by aperiodic fluctuations on a typical field scale  $B_c = \Phi_0 / W_{\text{eff}} L$  given by a flux quantum through the surface of the wires constituting the rings.  $W_{\text{eff}}$  includes a correction due to scattering on the edges of the wires in the limit where  $l_e > W$ ;  $W_{\text{eff}} = CW(W/l_e)^{1/2}$ , where  $C = 0.6$  (Ref. 26) for specular scattering. These results

TABLE I. Characteristics of the ring.  $W$  and  $l_e$  are deduced from weak localization measurements on wires etched in the same heterojunction with the same width. Note that the investigated frequency range between 2 and 20 GHz corresponds to a range of temperature between 0.1 and 1 K.

Mean perimeter of the ring $2L$	6 $\mu\text{m}$
Width $W$	0.2 $\mu\text{m}$
Effective width $W = 0.6W(W/l_e)^{1/2}$	0.07 $\mu\text{m}$
$l_e$	2 $\mu\text{m}$
$D = v_F l_e / 2$	0.2 $\text{m}^2 \text{s}^{-1}$
$\tau_D = L^2 / D$	$0.45 \times 10^{-10}$ s
$f_c = 1 / (2\pi\tau_D)$	3.5 GHz
$E_c = \hbar D / L^2$	170 mK
Phase coherence time $\tau_\phi$	$10^{-10}$ s

show that mesoscopic systems behave as diodes whose polarity depends on quantum interferences and can thus be inverted by applying a magnetic field or changing the rf frequency. The typical amplitude of the photovoltaic signal is 100 times larger than on metallic rings.<sup>8</sup> This difference can be easily related to the value of the resistance of GaAs samples, of the order of 6 k $\Omega$ , to be compared to several tens of  $\Omega$  for metallic samples. The maximum amplitude measured at the resonances of our experimental setup is of the order of  $0.3Re / \tau_D$  and only slightly varies with frequency for a given injected power on the resonances of our experimental setup. This weak frequency dependence of the PV voltage observed for frequencies much higher than  $f_c$  (see Fig. 5) is

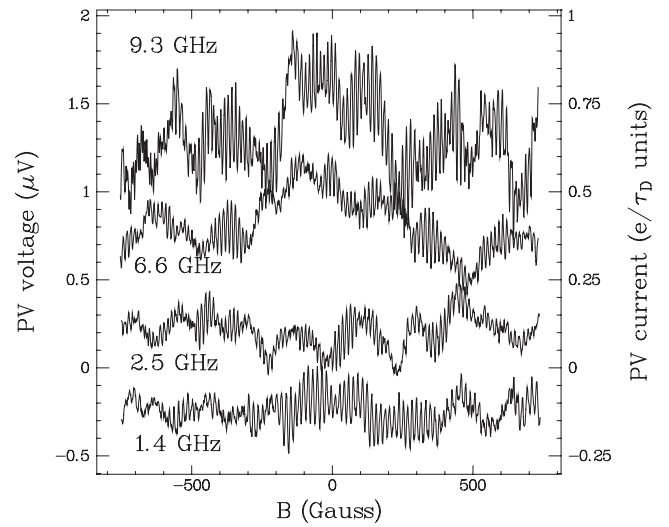


FIG. 4. PV voltage measured at  $T=30$  mK at several frequencies which correspond to the resonances of our experimental setup. The rf power at the generator level is  $-30$  dB and corresponds to an estimated injected power of 1 nW at the level of the AB ring. The signal exhibits an aperiodic component and a  $\Phi_0$  flux periodic oscillating part whose average on magnetic field is equal to zero. The right axis gives the value of the PV current  $I_{\text{PV}} = V_{\text{PV}} / R$  in units of  $e / \tau_D$  with  $R$  the resistance of the sample which is of the order of 6 k $\Omega$ . The different curves have been arbitrarily shifted along the  $Y$  axis for clarity purposes.

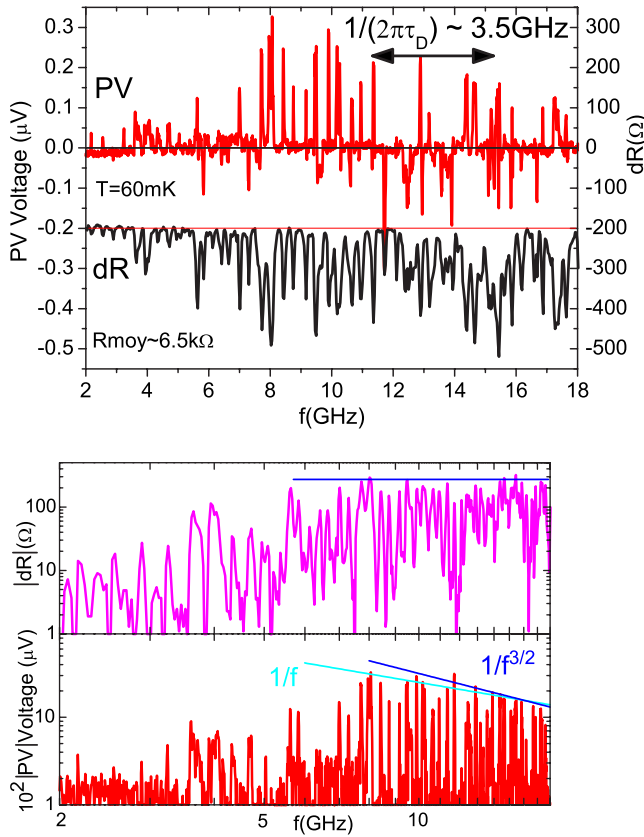


FIG. 5. (Color online) Frequency dependence of the photovoltaic voltage measured on the ring at  $T \approx 60$  mK and  $B=0$  G compared to the variation of the linear resistance. The peaks in the resistance are due to sample heating at the resonances of the cavity surrounding. Their amplitudes are nearly independent of frequency which indicates that the rf power sent to the sample is nearly the same on all these resonances above 6 GHz. In contrast, the PV voltage decreases at high frequency, in agreement with theoretical predictions  $1/f^{-3/2}$ . Note, however, that the experiment is not accurate enough to discriminate between a  $1/f^{-3/2}$  and a  $1/f$  decay.

compatible with theoretical predictions of Eq. (13) yielding a decay in  $1/f^{3/2}$  as will be discussed later.

The field dependent PV voltage is characterized by its UCF and AB components extracted from the area of the corresponding peaks in the Fourier transforms as shown on Fig. 6. We observe strong temperature dependences for UCF,  $h/e$ , and  $h/2e$  components which, to first approximation, can be described for all quantities by an exponential decay with a temperature scale of 200 mK which corresponds to the Thouless energy (see Fig. 7). The PV voltage nearly decreases by a factor of 10 between 0.1 and 0.5 K. This behavior is very different from what is observed in the same temperature range for similar quantities extracted from the dc magnetoconductance of the rings, as shown in the inset of Fig. 3. They are independent of temperature below 200 mK and exhibit at higher temperature a weak  $T^{-1/2}$  power law decay as  $\sqrt{E_c/k_B T}$  as observed in Reference 27, yielding a decrease by a factor of 3 up to 0.5 K. We do not have an explanation for the exponential decay observed for the PV voltage except that it presents a striking similarity to the temperature dependence of the imaginary component of the

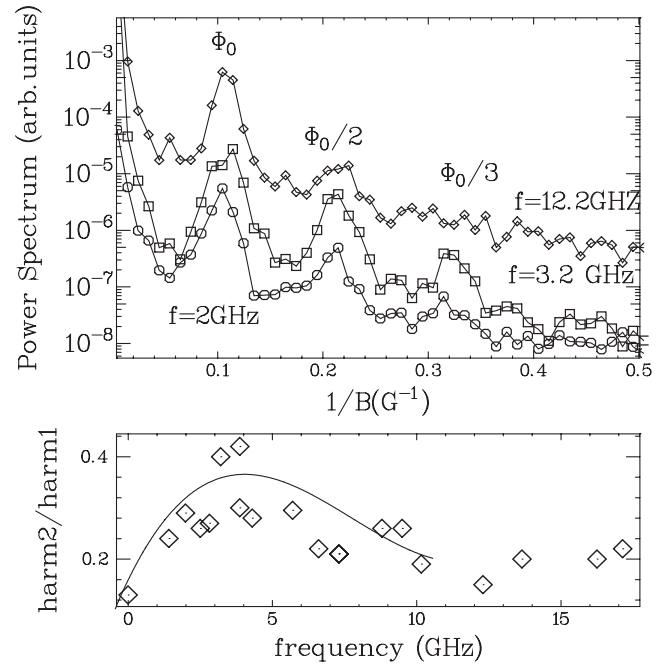


FIG. 6. Top: Square of the Fourier transform of the PV voltage of the ring for several frequencies at 30 mK. Bottom: Evolution of the ratio between the amplitudes of first and second harmonics  $H_2/H_1$ . The point at zero frequency was deduced from the second-harmonics response to low-frequency (30 Hz) excitations, like in Ref. 6 measured on the same ring. We observe that  $H_2/H_1$  goes through a broad maximum at  $\omega\tau_D \approx 1$ , which indicates a higher harmonics content of the PV voltage in this frequency range.

flux dependent ac conductance measured on isolated Aharonov-Bohm rings.<sup>28</sup>

The influence of the rf power was also investigated. Figure 8 displays the square of PV voltage as a function of the amplitude of the injected field in the rf lines at  $f = 3.84$  GHz. Note that due to our experimental setup, the amplitude of the rf field at the sample position is only known

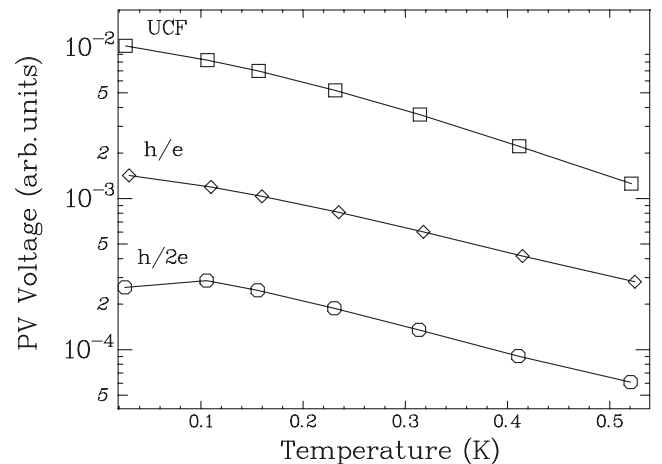


FIG. 7. Temperature dependence of PV voltage of the ring at 3.84 GHz. The periodic and aperiodic components of the signal exhibit an exponential decay above a characteristic temperature of the order of 200 mK  $\approx E_c$ .

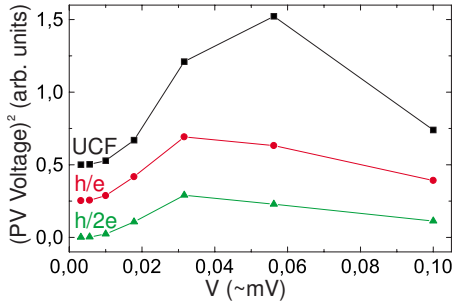


FIG. 8. (Color online) Dependence of the square of the PV voltage versus the amplitude of the rf field at 3.84 GHz. The curves are shifted for clarity.

within a numerical factor of the order of 3 or 4. The PV voltage quadratically increases at low rf field, goes through a maximum, and decreases at high rf power. There are different mechanisms which can explain this decrease: the amplitude of the induced rf voltage across the ring of the order of the Thouless energy together with induced dephasing and heating by the rf field.

IV. FIELD ASYMMETRY AND HARMONICS

It is important to note that the PV effect does not exhibit any particular magnetic field symmetry, in contrast with the two-wire linear resistance which is an even function of magnetic field. In the latter case, symmetry is a consequence of the Casimir-Onsager relations. As shown in Sec. II, there is no such expected symmetry for the PV effect, which is a second order nonlinear response, even if the measurement is also a two-wire measurement. The existence of a field asymmetry has been theoretically pointed out by Shutenko *et al.*<sup>29</sup>

and by Vavilov *et al.*<sup>30</sup> for mesoscopic pumping and PV effects and was observed experimentally in quantum dots.<sup>9</sup> We have shown in Sec. I how to relate this asymmetry either to the time reversal symmetry breaking induced by the high-frequency (HF) field or to electron-electron interactions at low frequency.<sup>20,21</sup>

Figure 9 shows the low field dependence of the PV voltage for various frequencies. One can see that for frequencies below 3 GHz, corresponding to  $\omega < 1/\tau_D$ , the phase of the Aharonov-Bohm oscillations is pinned either to 0 or to  $\pi$ . This was already observed in the measurements of the second order nonlinear conductance  $G_2$  in the very low frequency regime on rings similar to those investigated here.<sup>6</sup> It was shown that the main contribution in  $G_2^{AS}$ , the field anti-symmetric component of the second order conductance coefficient, is modulated by a UCF component linear on the characteristic field scale  $B_c$ . On the other hand, at higher frequencies the phase of the AB oscillations takes any value between 0 and  $\pi$  (see Fig. 9). We understand this behavior as the signature of time reversal symmetry breaking by the time dependent electric field (see Sec. II). It is interesting to note that in the same frequency region, the amplitude of the  $\phi_0/2$  component  $H_2$  of the PV voltage is of the order of magnitude of the first harmonics (see Fig. 6).  $H_2$  is indeed related to electronic diffusive trajectories encircling two times the ring. The typical diffusion time related to these trajectories  $\tau_D(2\text{loops})$  is equal to  $4\tau_D(1\text{loop})=4L^2/D$ . It was already pointed out in the dc limit<sup>6</sup> that the contribution of long trajectories is greater in the nonlinear mesoscopic transport compared to the linear one, giving rise to a higher harmonics content. This effect becomes more important at high frequency due to the contribution of  $I_{PV-}$  (see Fig. 1) with different frequency dependences for the  $\phi_0/2$  and  $\phi_0$  periodic contributions  $H_2$  and  $H_1$  increasing, respectively, like  $[\omega\tau_D(2\text{loops})]^2$  and  $[\omega\tau_D(1\text{loop})]^2$ . The ratio  $H_2/H_1$  is ex-

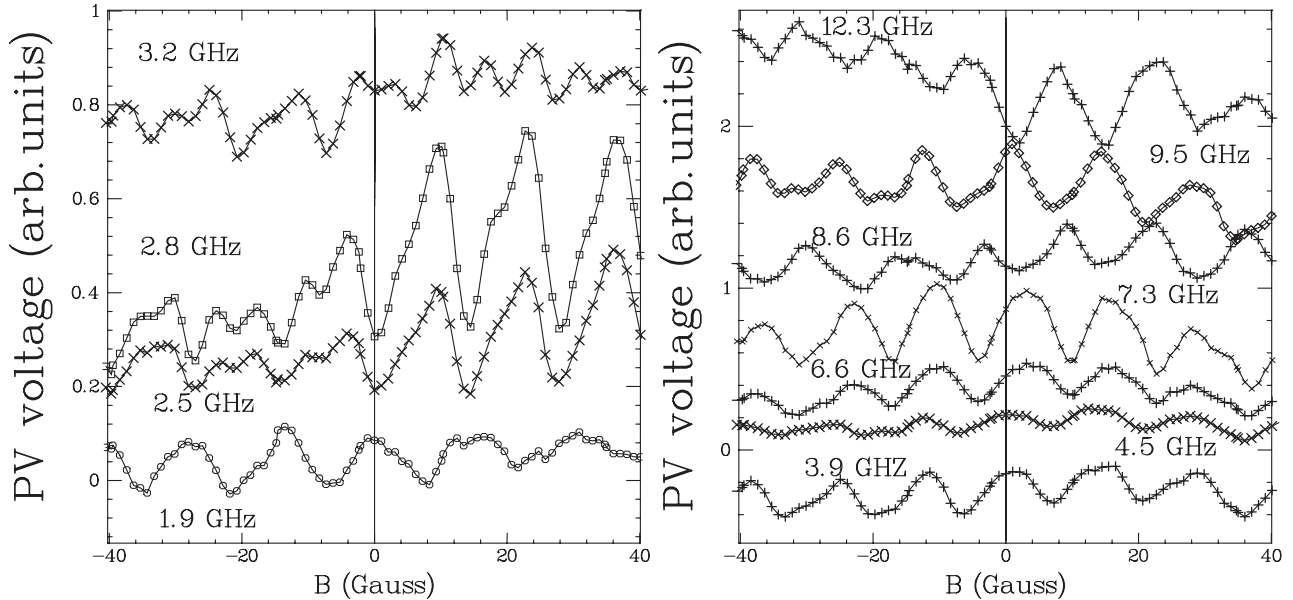


FIG. 9. Low field dependence of the photovoltaic voltage at several radio frequencies. Left:  $\omega \leq 1/\tau_D$ , the phase of the AB oscillations remains pinned to 0 or  $\pi$  at  $B=0$ . Right:  $\omega \geq 1/\tau_D$ , the phase of the AB oscillations takes any value between 0 and  $\pi$ . The vertical line in the plots corresponds to zero magnetic field. The curves have been shifted vertically for clarity.

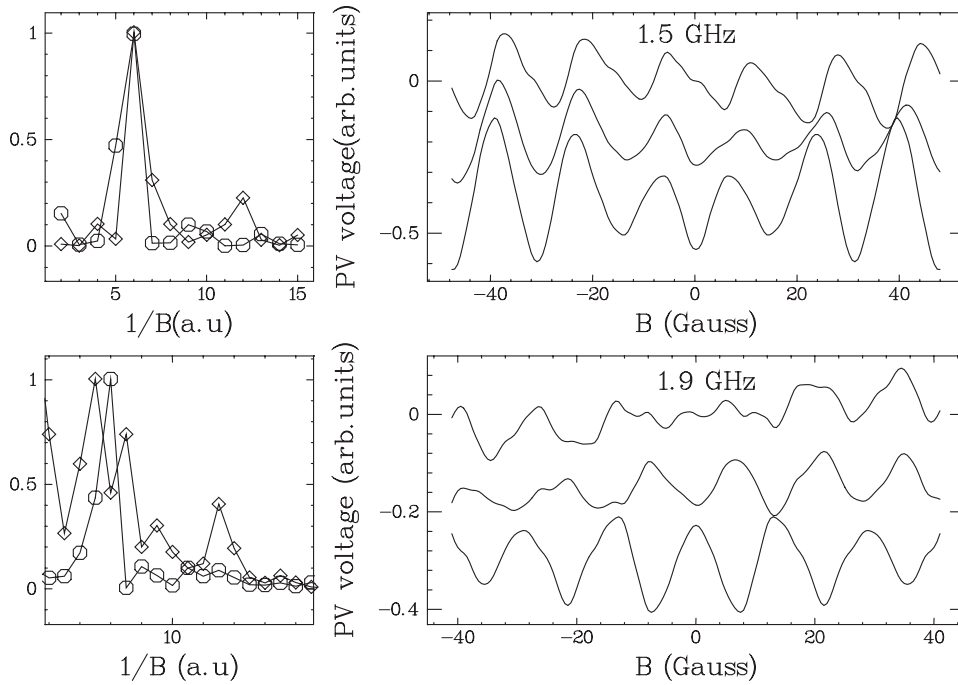


FIG. 10. Right: Decomposition of the low magnetic field dependence of the photovoltaic voltage (middle curves) at 1.5 and 1.9 GHz into a symmetrical (lower curve) and antisymmetrical (upper) curves. All curves are arbitrarily shifted for clarity purposes. Left: Fourier transforms of the symmetrical (circles) and antisymmetrical (diamonds) parts showing the large contribution of the  $\Phi_0/2$  harmonics present on the antisymmetrical data.

pected to increase by a factor of 2, go through a broad maximum at  $\omega\tau_D \approx 1$ , and decrease at higher frequency as observed in Fig. 6. It was possible to observe a clearer signature of this effect in the low field data ( $B \ll B_c$ ) where no signature of interactions induced asymmetry is observable. One can see in Fig. 10 that for  $f=1.5$  and 1.9 GHz corresponding to  $\omega\tau_D(2\text{loops}) \geq 1$  and  $\omega\tau_D(1\text{loop}) < 1$ , the second harmonics is only visible on the antisymmetric component on the PV voltage at low field related to  $I_{PV-}$ . From Eq. (11), one can deduce that the ratios between the second and first harmonics  $r_{S,AS} = H_2/H_1$  of the symmetrical and antisymmetrical components of the PV voltage are related by  $r_{AS} = r_S / (\omega\tau_D)^2 \gg r_S$  in this frequency range (see also Fig. 11). This effect disappears at higher frequency when  $\omega\tau_D \geq 1$  as expected. This shows that the PV voltage provides information on the diffusive motion of the electrons in the ring which is not contained in the low-frequency linear response. Moreover, we were able, by a thorough examination of the

asymmetry of the PV voltage at very low magnetic field, to distinguish between the contributions due to e-e interactions and due to the high frequency of the electric field. In the first case, the asymmetry is strongly modulated by UCF and does not show up in the vicinity of zero field. In the second case at  $\omega\tau_D > 1$ , the asymmetry is visible already at very low field.

#### V. FREQUENCY DEPENDENCE OF THE PV EFFECT: SIGNATURE OF RESONANT TWO LEVEL SYSTEMS?

As already shown in Fig. 5, the frequency dependence of  $V_{PV}$  exhibits a series of peaks of random sign and amplitude. The typical frequency spacing between these peaks is much smaller than  $f_c = 1/2\pi\tau_D \approx 3.6$  GHz. To first approximation, these peaks coincide with the rather broad resonance frequencies of our experimental setup. These are detected by measuring the effect of irradiation on the dc resistance of the sample, as shown on Fig. 12. (The decrease of resistance due to heating of the sample is simply proportional to the value of the rf electric field at the position of the sample.) The decrease of intensity of these PV voltage peaks at high frequency compared to  $f_c$  (see Fig. 5) can be approximately described by a power law  $f^{-x}$  with  $x = 1.25 \pm 0.25$ , in qualitative agreement with theoretical predictions  $1/f^{3/2}$  [Eq. (13)]. Below 6 GHz, most of the peaks observed coincide nearly exactly with the peaks observed on the resistance (see Fig. 12). However, it is important to note the existence of extra peaks on the photovoltaic signal, which are much narrower than the electromagnetic resonances on the linear resistance. This seems to indicate that the physical mechanisms involved in these peaks are different. The occurrence of these narrow peaks becomes more and more frequent when the rf increases, as shown in the bottom of Fig. 12. In Fig. 13, the field evolution of the frequency dependent PV voltage is plotted in a small frequency window. The peaks are clearly modulated in sign and intensity by the magnetic field, which

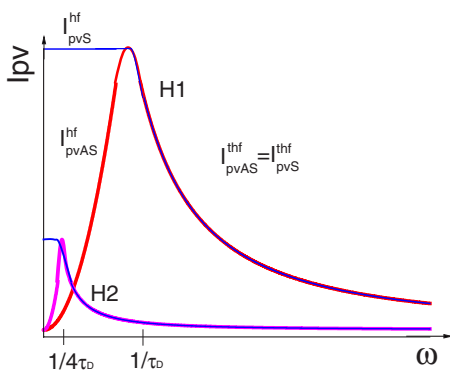


FIG. 11. (Color online) Expected frequency dependence of the components  $I_{PV+}$  and  $I_{PV-}$  of the PV current for  $H_1$  and  $H_2$  corresponding, respectively, to their first and second harmonics in  $\phi_0$  and  $\phi_0/2$ .

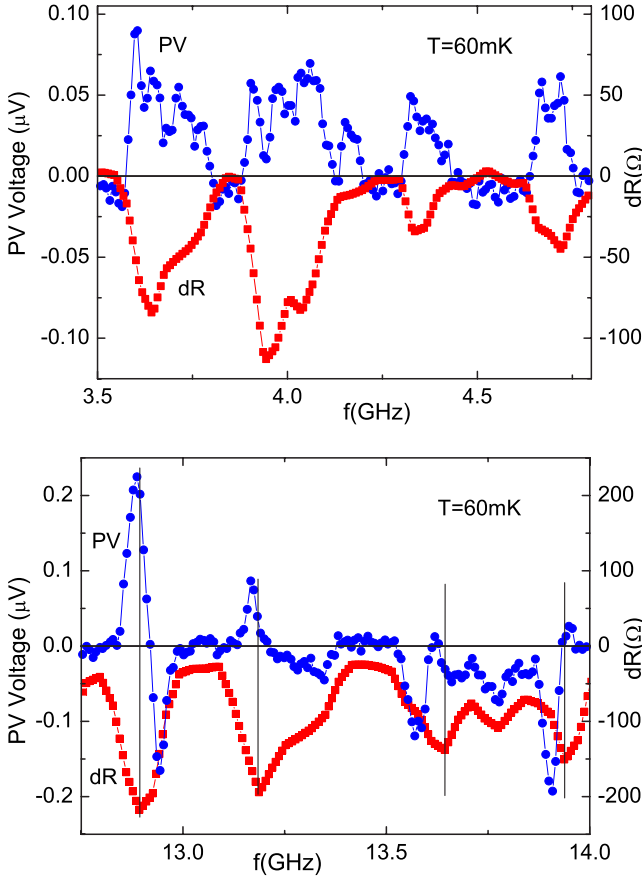


FIG. 12. (Color online) Zoom on the peaks in the PV voltage compared to the resonances of the electromagnetic environment of the sample detected on the linear resistance for two different frequency ranges. Note on the bottom graph, showing data between 12.5 and 13.5 GHz, the occurrence of sharp peaks in the PV voltage not present in the resistance. The two experiments were performed with a rf power of  $-35$  dB at the level of the generator.

indicates that they are sensitive to quantum interferences in the sample.

We propose in the following a possible explanation of these findings based on the resonant excitation of TLSs coupled to conduction electrons in the sample. These TLSs are probably related to metastable configurations of a scattering impurity having an excited state whose energy is close to the ground state.<sup>31,32</sup> Each of these TLSs behaves as a spin  $1/2$  in a magnetic field with a characteristic energy splitting  $\epsilon_i = \hbar\omega_i$  depending on its environment. It is very likely to bear a fluctuating electric dipolar moment of typical amplitude  $p_0 = ea_0$ , where  $a_0 = 10$  nm is the Bohr radius in GaAs. In the presence of a radio frequency electric field  $\vec{E}_{rf}$  of frequency  $\omega$ , a TLS located at point  $r_i$  can acquire an oscillating electric dipole  $\delta\vec{p}$  proportional to  $E_{rf}$  and exhibit a resonance when  $\omega = \omega_i$ ,

$$\delta\vec{p}(r_i, \omega) = \vec{E}_{rf}\alpha_0(T)\omega_i/\epsilon_0(\omega_i - \omega + i\gamma_i), \quad (14)$$

where  $\alpha_0(T) = \epsilon_0 p_0^2 / k_B T$  is the dc polarizability and  $\gamma_i$  is the decoherence rate of the TLS due to the dissipative coupling with its environment. Both  $\gamma_i$  and  $\omega_i$  depend on the interfer-

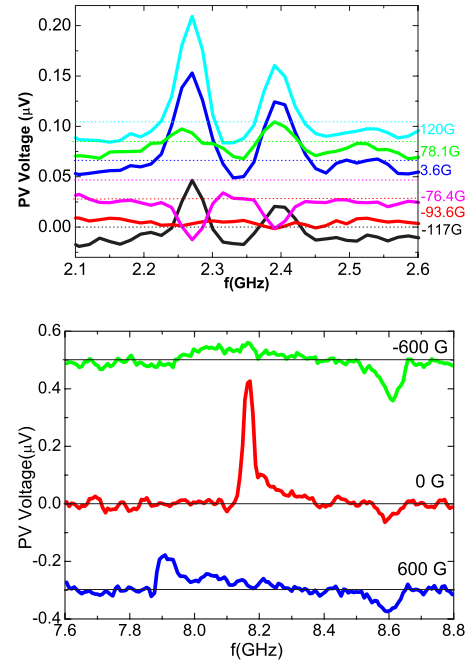


FIG. 13. (Color online) Frequency dependence of the PV voltage around 2 and 8 GHz measured at  $T=60$  and  $300$  mK for different magnetic fields. The curves are shifted for clarity. The zero is indicated by a horizontal line.

ence pattern of electronic wave functions at the point  $\vec{r}_i$ . At resonance when  $\omega_i/\gamma_i \approx 100$ , it is possible to obtain  $|\delta\vec{p}|$  nearly as large as  $p_0$ . This gives rise to a high-frequency oscillating contribution to the scattering potential  $dU_{dis}(r_i, \omega) \propto |\delta\vec{p}(r_i)|$  which also exhibits a resonance at  $\omega = \omega_i$ . Hence, the phase of the conduction electrons whose trajectories  $j$  visit the TLS at the point  $\vec{r}_i$  is changed by  $d\phi_j = \int_j (1/\hbar) dU_{dis}(r(t)) dt$  which can be of order 1.<sup>33</sup> As a result, the PV voltage  $V_{PV} \propto \langle \sum_j d\phi_j(t) E_{rf}(t) \rangle_t$  exhibits a pronounced peak at the frequency  $\omega_i$  undetectable, however, on the linear dc transport. The amplitude, sign, and width of this peak depend on the coupling of the TLS to the conduction electrons and are thus expected to exhibit mesoscopic fluctuations and Aharonov-Bohm oscillations as seen in the experiments. In other words, this would suggest that we can perform the spectroscopy of those coherent TLSs which are sufficiently coupled to the conduction electrons to be detected but not too much so that the decoherence rate is much smaller than their resonance frequency.

## VI. CONCLUSION

We have investigated the mesoscopic photovoltaic response of an Aharonov-Bohm ring to an electromagnetic wave between 1 and 18 GHz. The temperature, magnetic field, and rf amplitude dependences are in agreement with theoretical predictions. More precisely, we have shown that the rf evolution of the harmonics content and field asymmetry of the flux periodic part of the signal is rich in information on the diffusive motion of the electrons around the ring not contained in linear transport. We find that whereas the

low field AB oscillations are symmetric in low magnetic field at frequencies below  $f_c = 1/2\pi\tau_D$ , an asymmetry develops at higher frequency. This is due to the time reversal symmetry breaking induced by the time varying electric field. The longer the diffusive trajectories, the more pronounced this effect. As a result, the relative weight of the  $h/2e$  harmonics compared to the  $h/e$  one is larger on the field antisymmetric component than on the symmetric one. We also show that it is possible to distinguish between the field asymmetry of mesoscopic rectifications induced by electron-electron interactions (observed only at high magnetic field) from the asymmetry due to the high-frequency electric field. Finally, the observation of sharp peaks in the frequency dependence of the PV voltage is interpreted as the signature of individual two level systems at resonance with the rf electric field. This last result suggests the possibility of using PV voltage measurements for the detection of the electron spin resonance of magnetic moments in mesoscopic systems.

#### ACKNOWLEDGMENTS

We thank D. Mailly and B. Etienne for fabricating the GaAs/Ga<sub>1-x</sub>Al<sub>x</sub>As rings. We acknowledge fruitful discussions with N. Birge, M. Büttiker, M. Ferrier, G. Montambaux, M. Polianski, and C. Texier.

#### APPENDIX: CALCULATION OF $I_{PV+}$ AND $I_{PV-}$ USING SEMICLASSICS

In this section, we derive approximate expressions for  $I_{PV+}$  and  $I_{PV-}$  starting from the semiclassical expression of conductance. In order to treat the effects of the magnetic field, it is useful to write this expression in a form that directly leads to Onsager relations  $G(B) = G(-B)$  in the absence of microwave driving

$$G = \sum_{i,j} A_i A_j [\cos(\phi_j - \phi_i) + \cos(\phi_{-j} - \phi_{-i})]. \quad (\text{A1})$$

In this expression, the sum is taken on all possible classical trajectories leading from contact  $A$  to contact  $B$ . The trajectory  $-i$  is obtained by moving along the trajectory  $i$  in the opposite direction, and the phases  $\phi_i$  and  $\phi_{-i}$  are defined as the integral of the system's Lagrangian  $L(\mathbf{v}, \mathbf{r}, \tau)$ :

$$\begin{aligned} \phi_i &= \frac{1}{\hbar} \int_i L(\mathbf{v}(\tau), \mathbf{r}(\tau), \tau) d\tau \\ &= \frac{1}{\hbar} \int_i \left[ \frac{m\mathbf{v}^2(\tau)}{2} - e\mathbf{A}(\mathbf{r}(\tau), \tau)\mathbf{v}(\tau) + eV(\mathbf{r}(\tau), \tau) \right] d\tau, \end{aligned} \quad (\text{A2})$$

$$\phi_{-i} = \frac{1}{\hbar} \int_i L(-\mathbf{v}(\tau_i - \tau), \mathbf{r}(\tau_i - \tau), \tau) d\tau. \quad (\text{A3})$$

Here,  $V(\mathbf{r}, \tau)$  and  $\mathbf{A}(\mathbf{r}, \tau)$  are the scalar and vector potentials and  $\tau_i$  is the time needed to run from contact  $A$  to contact  $B$  along the trajectory  $i$ . In the case where the external fields are stationary, the particle energy is conserved and only tra-

jectories at the Fermi energy contribute to the conductance. If we assume now that the potential in the leads is stationary and that only the mesoscopic ring is exposed to microwave field, the particle energy is conserved inside the leads, but the initial energy in contact  $A$  can differ from the final energy in contact  $B$ . In the following, we will assume for simplicity that, as in the stationary case, the initial and final energies are both equal to the Fermi energy  $E_F$ . This approximation is questionable at very high frequency  $\omega\tau_D \gg 1$ .

In the presence of a static magnetic field  $\mathbf{B} = \text{rot } \mathbf{A} = \text{rot } \frac{\mathbf{B} \times \mathbf{r}}{2}$ , the phases are given by

$$\phi_i = \phi_i^0 + \alpha_i B, \quad \phi_{-i} = \phi_i^0 - \alpha_i B, \quad (\text{A4})$$

where  $\phi_i^0 = \frac{1}{\hbar} \int_i \frac{mv^2(\tau)}{2} d\tau$  and  $\alpha_i = \frac{e}{2\hbar} \int_i \mathbf{v}(\tau) \times \mathbf{r}(\tau) d\tau$ . By inserting these expressions into Eq. (A1), one can show that

$$G(V) = 2 \sum_{i,j} A_i A_j \cos(\phi_{ij}^0) \cos(\alpha_{ij} B), \quad (\text{A5})$$

with  $\phi_{ij}^0 = \phi_i^0 - \phi_j^0$  and  $\alpha_{ij} = \alpha_i - \alpha_j = 2\pi S_{ij} / \phi_0$ .

Under the influence of a radio frequency field, the values of the phases are changed by small increments  $\delta\phi_i, \delta\phi_{-i}$ :

$$\phi_i = \phi_i^0 + \alpha_i B + \delta\phi_i, \quad (\text{A6})$$

$$\phi_{-i} = \phi_i^0 - \alpha_i B + \delta\phi_{-i}. \quad (\text{A7})$$

At finite frequency, the increments  $\delta\phi_i$  and  $\delta\phi_{-i}$  are different, leading to the appearance of a component that is odd upon the inversion of magnetic field

$$\begin{aligned} G &= G_+ + G_- = \sum_{i,j} A_i A_j [\cos(\phi_{ij}^0 + \delta\phi_{ij}) \\ &\quad + \cos(\phi_{ij}^0 + \delta\phi_{-ij})] \cos(\alpha_{ij} B) - [\sin(\phi_{ij}^0 + \delta\phi_{ij}) \\ &\quad - \sin(\phi_{ij}^0 + \delta\phi_{-ij})] \sin(\alpha_{ij} B). \end{aligned}$$

First, we will estimate the amplitude of the photovoltaic current  $I_{PV+}$  even in magnetic field. In the limit of small phase shifts  $\delta\phi_i, \delta\phi_{-i}$ , we have

$$\begin{aligned} I_{PV+} &= \langle G_+ V \cos(\omega t) \rangle_t = -2V \left\langle \sum_{i,j} A_i A_j \sin(\delta\phi_{ij}^0) (\delta\phi_i + \delta\phi_{-i}) \right. \\ &\quad \left. \times \cos(\alpha_{ij} B) \cos(\omega t) \right\rangle_t. \end{aligned}$$

One has to estimate terms of the form

$$\begin{aligned} \langle \delta\phi_i \cos(\omega t) \rangle_t &= \left\langle \frac{e}{\hbar} \cos(\omega t) \int_t^{t+\tau_i} E_x \cos(\omega\tau) x_i(\tau) d\tau \right\rangle_t \\ &= -\frac{e}{2\hbar} \int_0^{\tau_i} E_x \cos(\omega\tau) x_i(\tau) d\tau \\ &\sim \frac{eV \sin(\omega\tau_i)}{\hbar \omega}, \end{aligned} \quad (\text{A8})$$

where  $x_i(\tau)$  is the  $x$  coordinate of the  $i$ th trajectory,  $\tau_i$  is the time needed to go from point  $A$  to point  $B$ , and  $V = E_x |AB|$  is the ac voltage. A similar estimate holds for  $\delta\phi_{-i}$ , leading to

$$I_{PV+} \sim \frac{eV^2}{\hbar} \sum_{ij} A_i A_j \sin(\phi_j - \phi_i) \cos(\alpha_{ij} B) \frac{\sin(\omega \tau_i)}{\omega}. \quad (\text{A9})$$

In the high-frequency region  $\omega \tau_D \gg 1$ ,  $\sin(\omega \tau_i)$  is essentially a random phase, and leads [similar to  $\cos(\alpha_{ij} B)$ ] to conductance fluctuations of the order  $\frac{e^2}{\hbar \sqrt{\omega \tau_D}}$  at high frequency.<sup>19</sup> Hence,

$$I_{PV+} \sim \frac{e^3 V^2}{\hbar^2 \omega \sqrt{\omega \tau_D}} \quad (\omega \tau_D \gg 1). \quad (\text{A10})$$

In the low-frequency regime, the quantity  $\sin(\omega \tau_i)/\omega \sim \tau_i$  has fluctuations of the order  $\tau_D$  around its average value, and the conductance fluctuations are of the order  $\frac{e^2}{\hbar}$ ; therefore,

$$I_{PV+} \sim \frac{e^3 V^2 \tau_D}{\hbar^2} \quad (\omega \tau_D \ll 1). \quad (\text{A11})$$

The term antisymmetric in  $B$  is zero in the absence of rf field:

$$\begin{aligned} G_- &= \sum_{ij} A_i A_j \cos(\phi_{j,i,0}) \sin(\alpha_{j,i} B) (\delta \phi_{j,i} - \delta \phi_{-j,-i}) \\ &= 2 \sum_{ij} A_i A_j \cos(\phi_{j,i,0}) \sin(\alpha_{j,i} B) (\delta \phi_j - \delta \phi_{-j}). \end{aligned} \quad (\text{A12})$$

In the presence of rf field, the component of the photovoltaic current antisymmetric in field is calculated from

$$I_{PV-} = \langle G_- V \cos(\omega t) \rangle_t = \left\langle 2V \sum_{ij} A_i A_j \cos(\phi_{j,i,0}) \sin(\alpha_{j,i} B) \times [\delta \phi_i(t) - \delta \phi_{-i}(t)] \cos(\omega t) \right\rangle_t,$$

$$\begin{aligned} \delta \phi_i(t) - \delta \phi_{-i}(t) &= \frac{-eE_x}{\hbar} \int_0^{\tau_i} d\tau x(\tau) \{ \cos(\omega \tau + \omega t) \\ &\quad - \cos[\omega(\tau_i - \tau) + \omega t] \}. \end{aligned}$$

This leads to a term in  $\sin(\omega t)$  and a term in  $\cos(\omega t)$ . When calculating  $I_{PV-} = \langle \delta G_-(V(t)) V \cos(\omega t) \rangle_t$ , we keep only the term in  $\cos(\omega t)$ . This means that we have neglected the

imaginary component of the linear conductance induced at finite frequency by quantum interferences.<sup>16</sup>

$$\begin{aligned} &\langle (\delta \phi_i - \delta \phi_{-i}) \cos(\omega t) \rangle_t \\ &= \frac{eE_x}{\hbar} \sin(\omega \tau_i/2) \int_0^{\tau_i} d\tau x(\tau) \sin[\omega(\tau - \tau_i/2)] \\ &\sim \sin(\omega \tau_i/2) \sqrt{(\delta \phi)^2}. \end{aligned} \quad (\text{A13})$$

In the following equations we detail the calculation of the mean square phase difference  $\langle (\delta \phi)^2 \rangle$  inspired by Ref. 15.

$$\begin{aligned} \langle (\delta \phi)^2 \rangle &= \frac{(eE_x)^2}{\hbar^2} \int_0^{\tau_1} \int_0^{\tau_2} d\tau_1 d\tau_2 \sin[\omega(\tau_1 - \tau_2/2)] \\ &\quad \times \sin[\omega(\tau_2 - \tau_1/2)] \langle x(\tau_1) x(\tau_2) \rangle \\ &= \frac{(eE_x)^2}{\hbar^2} \int_0^{\tau_1} \int_0^{\tau_2} d\tau_1 d\tau_2 \sin[\omega(\tau_1 - \tau_1/2)] \\ &\quad \times \sin[\omega(\tau_2 - \tau_1/2)] D \min(\tau_1, \tau_2) \\ &= \frac{(eE_x)^2 D}{\hbar^2} \frac{2\omega \tau_i [2 + \cos(2\omega \tau_i)] - 3 \sin(2\omega \tau_i)}{2\omega^3}. \end{aligned} \quad (\text{A14})$$

In the low-frequency limit  $\omega t \rightarrow 0$ , we recover the result of Ref. 15. In the high-frequency regime,  $\omega t \gg 1$ ,  $\langle \delta \phi^2 \rangle$  decays  $\propto 1/\omega^2$ .

Omitting numerical factors,

$$\langle (\delta \phi)^2 \rangle \sim \frac{(eE_x \omega)^2 D \tau_D^5}{\hbar^2}, \quad \omega \tau_D \ll 1, \quad (\text{A15})$$

$$\langle (\delta \phi)^2 \rangle \sim \frac{(eE_x)^2 D \tau_D}{\omega^2 \hbar^2}, \quad \omega \tau_D \gg 1, \quad (\text{A16})$$

where  $\tau_D$  is the mean diffusion time in the ring. We then have in the low-frequency regime

$$I_{PV-} \sim V \frac{e^2}{\hbar} \omega \tau_D \sqrt{\frac{(eV\omega)^2 \tau_D^4}{\hbar^2}} \sim \frac{e^3 V^2}{\hbar^2} \omega^2 \tau_D^3 \quad (\text{A17})$$

and in the high-frequency regime

$$I_{PV-} \sim V \frac{e^2}{\hbar \sqrt{\omega \tau_D}} \sqrt{\frac{(eV)^2}{\omega^2 \hbar^2}} \sim \frac{e^3 V^2}{\hbar^2 \omega \sqrt{\omega \tau_D}}. \quad (\text{A18})$$

<sup>1</sup>See, e.g., *Mesoscopic Phenomena in Solids*, edited by B. L. Altshuler, P. A. Lee, and R. A. Webb (Elsevier, Amsterdam, 1991); Y. Imry, *Introduction to Mesoscopic Physics* (Oxford University Press, New York, 1997).

<sup>2</sup>B. L. Altshuler and D. E. Khmel'nitskii, JETP Lett. **42**, 359 (1985); A. I. Larkin and D. E. Khmel'nitskii, Sov. Phys. JETP **64**, 1075 (1986).

<sup>3</sup>J. Wei, M. Shimogawa, Z. Wang, I. Radu, R. Dormaier, and D. H. Cobden, Phys. Rev. Lett. **95**, 256601 (2005).

<sup>4</sup>R. Leturcq, D. Sanchez, G. Gotz, T. Ihn, K. Ensslin, D. C.

Driscoll, and A. C. Gossard, Phys. Rev. Lett. **96**, 126801 (2006).

<sup>5</sup>D. M. Zumbühl, C. M. Marcus, M. P. Hanson, and A. C. Gossard, Phys. Rev. Lett. **96**, 206802 (2006).

<sup>6</sup>L. Angers, E. Zakka-Bajjani, R. Deblock, S. Guéron, H. Bouchiat, A. Cavanna, U. Gennser, and M. Polianski, Phys. Rev. B **75**, 115309 (2007).

<sup>7</sup>A. Bykov, G. Gusev, and Z. Kvon, Pis'ma Zh. Eksp. Teor. Fiz. **49**, 13 (1989) [JETP Lett. **49**, 13 (1989)].

<sup>8</sup>R. E. Bartolo, N. Giordano, X. Huang, and G. H. Bernstein, Phys.

- Rev. B **55**, 2384 (1997).
- <sup>9</sup>L. DiCarlo, C. M. Marcus, and J. S. Harris, Phys. Rev. Lett. **91**, 246804 (2003).
- <sup>10</sup>V. Fal'ko and D. Khmel'niskii, Zh. Eksp. Teor. Fiz. **95**, 328 (1989) [Sov. Phys. JETP **68**, 186 (1989)].
- <sup>11</sup>B. Spivak, F. Zhou, and M. T. Beal Monod, Phys. Rev. B **51**, 13226 (1995).
- <sup>12</sup>P. W. Brouwer, Phys. Rev. B **63**, 121303(R) (2001).
- <sup>13</sup>M. Moskalets and M. Büttiker, Phys. Rev. B **69**, 205316 (2004).
- <sup>14</sup>K. Richter, D. Ullmo, and R. A. Jalabert, Phys. Rev. B **54**, R5219 (1996).
- <sup>15</sup>B. L. Altshuler, A. G. Aronov, and D. E. Khmel'nitskii, Solid State Commun. **39**, 619 (1981).
- <sup>16</sup>In principle, one should take into account the imaginary component  $\Im G$  of the quantum conductance predicted by A. G. Aronov and Yu. V. Sharvin, Rev. Mod. Phys. **59**, 755 (1987) and observed experimentally by John B. Pieper and John C. Price, Phys. Rev. Lett. **72**, 3586 (1994).  $\Im G$  is proportional to  $\omega\tau_D$  in the frequency range considered here. This would yield another contribution also proportional to  $(\omega\tau_D)^2$ , i.e., of the same order as those discussed in the following.
- <sup>17</sup>V. E. Kravtsov and V. I. Yudson, Phys. Rev. Lett. **70**, 210 (1993); A. G. Aronov and V. E. Kravtsov, Phys. Rev. B **47**, 13409 (1993).
- <sup>18</sup>J. Liu, M. A. Pennington, and N. Giordano, Phys. Rev. B **45**, 1267 (1992); A. Bykov, Z. Kvon, L. Litvin, Y. V. Nastaushev, V. Mansurov, V. Migal', and S. Moshchenko, Pis'ma Zh. Eksp. Teor. Fiz. **58**, 538 (1993) [JETP Lett. **58**, 543 (1993)]; J. Wei, S. Pereverzev, and M. E. Gershenson, Phys. Rev. Lett. **96**, 086801 (2006).
- <sup>19</sup>D. Z. Liu, Ben Yu-Kuang Hu, C. A. Stafford, and S. Das Sarma, Phys. Rev. B **50**, 5799 (1994).
- <sup>20</sup>D. Sanchez and M. Büttiker, Phys. Rev. Lett. **93**, 106802 (2004); Int. J. Quantum Chem. **105**, 906 (2005).
- <sup>21</sup>B. Spivak and A. Zyuzin, Phys. Rev. Lett. **93**, 226801 (2004); E. Deyo, B. Spivak, and A. Zyuzin, Phys. Rev. B **74**, 104205 (2006).
- <sup>22</sup>M. L. Polianski and M. Büttiker, Phys. Rev. Lett. **96**, 156804 (2006).
- <sup>23</sup>P. W. Brouwer, Phys. Rev. B **58**, R10135 (1998).
- <sup>24</sup>M. Switkes, C. Marcus, K. Campman, and A. Gossard, Science **283**, 1905 (1999).
- <sup>25</sup>L. Onsager, Phys. Rev. **38**, 2265 (1931); H. G. B. Casimir, Rev. Mod. Phys. **17**, 343 (1945).
- <sup>26</sup>C. W. J. Beenakker and H. van Houten, Phys. Rev. B **38**, 3232 (1988).
- <sup>27</sup>S. Washburn and R. A. Webb, Adv. Phys. **35**, 375 (1986).
- <sup>28</sup>R. Deblock, Y. Noat, H. Bouchiat, B. Reulet, and D. Mailly, Phys. Rev. Lett. **84**, 5379 (2000).
- <sup>29</sup>T. A. Shutenko, I. L. Aleiner, and B. L. Altshuler, Phys. Rev. B **61**, 10366 (2000).
- <sup>30</sup>M. G. Vavilov, V. Ambegaokar, and I. L. Aleiner, Phys. Rev. B **63**, 195313 (2001).
- <sup>31</sup>F. Pierre, A. B. Gougam, A. Anthore, H. Pothier, D. Esteve, and Norman O. Birge, Phys. Rev. B **68**, 085413 (2003).
- <sup>32</sup>A. Zawadowski, Jan von Delft, and D. C. Ralph, Phys. Rev. Lett. **83**, 2632 (1999).
- <sup>33</sup>S. Feng, P. A. Lee, and A. D. Stone, Phys. Rev. Lett. **56**, 1960 (1986).